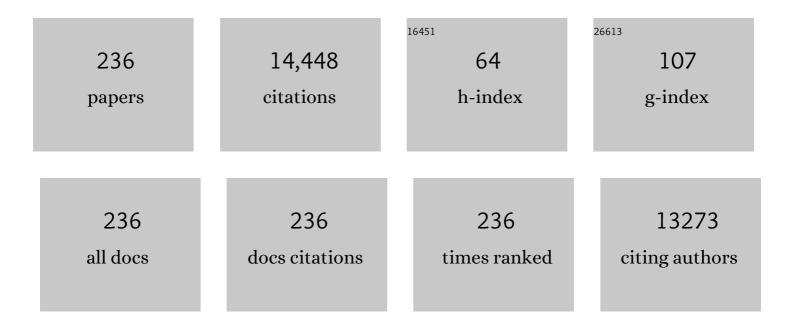
List of Publications by Year in descending order

Source: https://exaly.com/author-pdf/3787942/publications.pdf Version: 2024-02-01



#	Article	IF	CITATIONS
1	The enhancement of CdS photocatalytic activity for water splitting via anti-photocorrosion by coating Ni2P shell and removing nascent formed oxygen with artificial gill. Applied Catalysis B: Environmental, 2018, 221, 243-257.	20.2	371
2	5.1% Apparent quantum efficiency for stable hydrogen generation over eosin-sensitized CuO/TiO2 photocatalyst under visible light irradiation. Catalysis Communications, 2007, 8, 1267-1273.	3.3	361
3	Eosin Y-sensitized graphitic carbon nitride fabricated by heating urea for visible light photocatalytic hydrogen evolution: the effect of the pyrolysis temperature of urea. Physical Chemistry Chemical Physics, 2013, 15, 7657.	2.8	332
4	Sites for High Efficient Photocatalytic Hydrogen Evolution on a Limited-Layered MoS ₂ Cocatalyst Confined on Graphene Sheets―The Role of Graphene. Journal of Physical Chemistry C, 2012, 116, 25415-25424.	3.1	323
5	Synthesis of CdS Nanorods by an Ethylenediamine Assisted Hydrothermal Method for Photocatalytic Hydrogen Evolution. Journal of Physical Chemistry C, 2009, 113, 9352-9358.	3.1	296
6	Enhanced Electron Transfer from the Excited Eosin Y to mpg-C ₃ N ₄ for Highly Efficient Hydrogen Evolution under 550 nm Irradiation. Journal of Physical Chemistry C, 2012, 116, 19644-19652.	3.1	284
7	Peculiar synergetic effect of MoS 2 quantum dots and graphene on Metal-Organic Frameworks for photocatalytic hydrogen evolution. Applied Catalysis B: Environmental, 2017, 210, 45-56.	20.2	269
8	Photocatalytic and photoelectric properties of cubic Ag3PO4 sub-microcrystals with sharp corners and edges. Chemical Communications, 2012, 48, 3748.	4.1	268
9	Dye-Sensitized Reduced Graphene Oxide Photocatalysts for Highly Efficient Visible-Light-Driven Water Reduction. Journal of Physical Chemistry C, 2011, 115, 13938-13945.	3.1	265
10	Photocorrosion inhibition of CdS-based catalysts for photocatalytic overall water splitting. Nanoscale, 2020, 12, 1213-1223.	5.6	265
11	Visible Photocatalytic Water Splitting and Photocatalytic Two-Electron Oxygen Formation over Cu- and Fe-Doped g-C ₃ N ₄ . Journal of Physical Chemistry C, 2016, 120, 56-63.	3.1	251
12	Direct Observation of Charge Separation on Anatase TiO2 Crystals with Selectively Etched {001} Facets. Journal of the American Chemical Society, 2016, 138, 2917-2920.	13.7	210
13	Enhancing catalytic activity and stability for CO ₂ methanation on Ni@MOF-5 via control of active species dispersion. Chemical Communications, 2015, 51, 1728-1731.	4.1	209
14	Selective growth of Ag3PO4 submicro-cubes on Ag nanowires to fabricate necklace-like heterostructures for photocatalytic applications. Journal of Materials Chemistry, 2012, 22, 14847.	6.7	179
15	Inhibition of photocorrosion of CdS via assembling with thin film TiO 2 and removing formed oxygen by artificial gill for visible light overall water splitting. Applied Catalysis B: Environmental, 2017, 212, 129-139.	20.2	168
16	Inhibition of CdS photocorrosion by Al2O3 shell for highly stable photocatalytic overall water splitting under visible light irradiation. Applied Catalysis B: Environmental, 2018, 226, 373-383.	20.2	167
17	Dye-Sensitized NiS _{<i>x</i>} Catalyst Decorated on Graphene for Highly Efficient Reduction of Water to Hydrogen under Visible Light Irradiation. ACS Catalysis, 2014, 4, 2763-2769.	11.2	163
18	Investigation of the steam reforming of a series of model compounds derived from bio-oil for hydrogen production. Applied Catalysis B: Environmental, 2009, 88, 376-385.	20.2	157

#	Article	IF	CITATIONS
19	Investigation of steam reforming of acetic acid to hydrogen over Ni–Co metal catalyst. Journal of Molecular Catalysis A, 2007, 261, 43-48.	4.8	155
20	Photocatalytic production of hydrogen in single component and mixture systems of electron donors and monitoring adsorption of donors by in situ infrared spectroscopy. Chemosphere, 2003, 52, 843-850.	8.2	154
21	Eosin Y-sensitized nitrogen-doped TiO2 for efficient visible light photocatalytic hydrogen evolution. Journal of Molecular Catalysis A, 2008, 282, 117-123.	4.8	150
22	Highly efficient hydrogen evolution over Co(OH)2 nanoparticles modified g-C3N4 co-sensitized by Eosin Y and Rose Bengal under Visible Light Irradiation. Applied Catalysis B: Environmental, 2016, 188, 56-64.	20.2	150
23	Small-sized Ni(1 1 1) particles in metal-organic frameworks with low over-potential for visible photocatalytic hydrogen generation. Applied Catalysis B: Environmental, 2016, 190, 12-25.	20.2	145
24	Photocatalytic hydrogen generation in the presence of chloroacetic acids over Pt/TiO2. Chemosphere, 2006, 63, 1312-1318.	8.2	139
25	Concave trisoctahedral Ag ₃ PO ₄ microcrystals with high-index facets and enhanced photocatalytic properties. Chemical Communications, 2013, 49, 636-638.	4.1	137
26	Visible-Light-Induced Photocatalytic Hydrogen Generation on Dye-Sensitized Multiwalled Carbon Nanotube/Pt Catalyst. Journal of Physical Chemistry C, 2007, 111, 11494-11499.	3.1	132
27	The effect of impregnation strategy on structural characters and CO2 methanation properties over MgO modified Ni/SiO2 catalysts. Catalysis Communications, 2014, 54, 55-60.	3.3	132
28	Comparative study of alumina-supported transition metal catalysts for hydrogen generation by steam reforming of acetic acid. Applied Catalysis B: Environmental, 2010, 99, 289-297.	20.2	131
29	Unveiling the Activity and Stability Origin of BiVO ₄ Photoanodes with FeNi Oxyhydroxides for Oxygen Evolution. Angewandte Chemie - International Edition, 2020, 59, 18990-18995.	13.8	129
30	The Doping Effect of Bi on TiO ₂ for Photocatalytic Hydrogen Generation and Photodecolorization of Rhodamine B. Journal of Physical Chemistry C, 2009, 113, 9950-9955.	3.1	127
31	Boron and nitrogen co-doped titania with enhanced visible-light photocatalytic activity for hydrogen evolution. Applied Surface Science, 2008, 254, 6831-6836.	6.1	126
32	Fabrication of Low Adsorption Energy Ni–Mo Cluster Cocatalyst in Metal–Organic Frameworks for Visible Photocatalytic Hydrogen Evolution. ACS Applied Materials & Interfaces, 2016, 8, 10808-10819.	8.0	124
33	Photocatalytic hydrogen evolution over Pt/Cd0.5Zn0.5S from saltwater using glucose as electron donor: An investigation of the influence of electrolyte NaCl. International Journal of Hydrogen Energy, 2011, 36, 4291-4297.	7.1	123
34	Dye-cosensitized graphene/Pt photocatalyst for high efficient visible light hydrogen evolution. International Journal of Hydrogen Energy, 2012, 37, 10564-10574.	7.1	121
35	Enhancing activity for carbon dioxide methanation by encapsulating (1 1 1) facet Ni particle in metal–organic frameworks at low temperature. Journal of Catalysis, 2017, 348, 200-211.	6.2	118
36	Improved quantum yield for photocatalytic hydrogen generation under visible light irradiation over eosin sensitized TiO2—Investigation of different noble metal loading. Journal of Molecular Catalysis A, 2006, 259, 275-280.	4.8	117

#	Article	IF	CITATIONS
37	Direct electrochemistry and electrocatalysis of hemoglobin immobilized on carbon paste electrode by silica sol–gel film. Biosensors and Bioelectronics, 2004, 19, 1269-1275.	10.1	113
38	Formation of multilayer-Eosin Y-sensitized TiO2 via Fe3+ coupling for efficient visible-light photocatalytic hydrogen evolution. International Journal of Hydrogen Energy, 2009, 34, 5629-5636.	7.1	111
39	Facile synthesis of tetrahedral Ag3PO4 submicro-crystals with enhanced photocatalytic properties. Journal of Materials Chemistry A, 2013, 1, 2387.	10.3	109
40	Nitrogen-incorporation activates NiFeOx catalysts for efficiently boosting oxygen evolution activity and stability of BiVO4 photoanodes. Nature Communications, 2021, 12, 6969.	12.8	109
41	Steam reforming of acetic acid over Ni/ZrO2 catalysts: Effects of nickel loading and particle size on product distribution and coke formation. Applied Catalysis A: General, 2012, 417-418, 281-289.	4.3	107
42	Selective Growth of Metallic Ag Nanocrystals on Ag ₃ PO ₄ Submicro ubes for Photocatalytic Applications. Chemistry - A European Journal, 2012, 18, 14272-14275.	3.3	100
43	High-Efficient Photocatalytic Hydrogen Evolution on Eosin Y-Sensitized Tiâ ^{~,} MCM41 Zeolite under Visible-Light Irradiation. Journal of Physical Chemistry C, 2007, 111, 8237-8241.	3.1	97
44	Enhancement of photocatalytic activity of cadmium sulfide for hydrogen evolution by photoetching. International Journal of Hydrogen Energy, 2008, 33, 2007-2013.	7.1	97
45	Two-dimensional dendritic Ag3PO4 nanostructures and their photocatalytic properties. Physical Chemistry Chemical Physics, 2012, 14, 14486.	2.8	92
46	The role of a metallic copper interlayer during visible photocatalytic hydrogen generation over a Cu/Cu ₂ O/Cu/TiO ₂ catalyst. Catalysis Science and Technology, 2017, 7, 5028-5037.	4.1	92
47	Visible-light-driven photoelectrochemical and photocatalytic performances of Cr-doped SrTiO3/TiO2 heterostructured nanotube arrays. Scientific Reports, 2013, 3, 2720.	3.3	91
48	Modulating and controlling active species dispersion over Ni–Co bimetallic catalysts for enhancement of hydrogen production of ethanol steam reforming. International Journal of Hydrogen Energy, 2016, 41, 3349-3362.	7.1	91
49	Catalytic CO oxidation over palladium supported NaZSM-5 catalysts. Applied Catalysis B: Environmental, 2003, 41, 279-286.	20.2	88
50	Ni-Mo-S nanoparticles modified graphitic C3N4 for efficient hydrogen evolution. Applied Surface Science, 2018, 427, 587-597.	6.1	88
51	Uniformly Sized (112) Facet Co ₂ P on Graphene for Highly Effective Photocatalytic Hydrogen Evolution. Journal of Physical Chemistry C, 2016, 120, 6409-6415.	3.1	86
52	The Role of Cu(I) Species for Photocatalytic Hydrogen Generation Over CuO x /TiO2. Catalysis Letters, 2009, 133, 97-105.	2.6	84
53	Phosphate-assisted hydrothermal synthesis of hexagonal CdS for efficient photocatalytic hydrogen evolution. CrystEngComm, 2012, 14, 6974.	2.6	84
54	Robust Pt–Sn alloy decorated graphene nanohybrid cocatalyst for photocatalytic hydrogen evolution. Chemical Communications, 2014, 50, 9281-9283.	4.1	84

#	Article	IF	CITATIONS
55	Efficient Photocatalytic Hydrogen Evolution from Water without an Electron Mediator over Ptâ^'Rose Bengal Catalysts. Journal of Physical Chemistry C, 2009, 113, 2630-2635.	3.1	83
56	Enhancing catalytic activity and stability for CO ₂ methanation on Ni–Ru/l³-Al ₂ O ₃ via modulating impregnation sequence and controlling surface active species. RSC Advances, 2014, 4, 16472-16479.	3.6	80
57	Functionalization of TiO2 with graphene quantum dots for efficient photocatalytic hydrogen evolution. Superlattices and Microstructures, 2016, 94, 237-244.	3.1	77
58	Metal-free plasmonic boron phosphide/graphitic carbon nitride with core-shell structure photocatalysts for overall water splitting. Applied Catalysis B: Environmental, 2021, 280, 119410.	20.2	75
59	Inhibition of methane formation in steam reforming reactions through modification of Ni catalyst and the reactants. Green Chemistry, 2009, 11, 724.	9.0	74
60	Acetic acid steam reforming to hydrogen over Co–Ce/Al2O3 and Co–La/Al2O3 catalysts—The promotion effect of Ce and La addition. Catalysis Communications, 2010, 12, 50-53.	3.3	74
61	The difference of roles of alkaline-earth metal oxides on silica-supported nickel catalysts for CO ₂ methanation. RSC Advances, 2014, 4, 58171-58177.	3.6	71
62	Inhibition of hydrogen and oxygen recombination using oxygen transfer reagent hemin chloride in Pt/TiO2 dispersion for photocatalytic hydrogen generation. Applied Catalysis B: Environmental, 2017, 203, 408-415.	20.2	68
63	Bio-oil steam reforming, partial oxidation or oxidative steam reforming coupled with bio-oil dry reforming to eliminate CO2 emission. International Journal of Hydrogen Energy, 2010, 35, 7169-7176.	7.1	67
64	Highly efficient hydrogen production from alkaline aldehyde solutions facilitated by palladium nanotubes. Nano Energy, 2014, 8, 103-109.	16.0	67
65	Synthesis of silver nanowires with different aspect ratios as alcohol-tolerant catalysts for oxygen electroreduction. Electrochemistry Communications, 2008, 10, 1027-1030.	4.7	66
66	Visible-light driven photocatalytic hydrogen generation on Eosin Y-sensitized Pt-loaded nanotube Na2Ti2O4(OH)2. Journal of Molecular Catalysis A, 2007, 266, 75-79.	4.8	63
67	Nano-Cu catalyze hydrogen production from formaldehyde solution at room temperature. International Journal of Hydrogen Energy, 2008, 33, 2225-2232.	7.1	63
68	Steam reforming of acetic acid over cobalt catalysts: Effects of Zr, Mg and K addition. International Journal of Hydrogen Energy, 2017, 42, 4793-4803.	7.1	63
69	Distinctive organized molecular assemble of MoS ₂ , MOF and Co ₃ O ₄ , for efficient dye-sensitized photocatalytic H ₂ evolution. Catalysis Science and Technology, 2018, 8, 2352-2363.	4.1	63
70	Facile and Rapid Oxidation Fabrication of BiOCl Hierarchical Nanostructures with Enhanced Photocatalytic Properties. Chemistry - A European Journal, 2013, 19, 9472-9475.	3.3	62
71	Super-paramagnetic nano-Fe ₃ O ₄ /graphene for visible-light-driven hydrogen evolution. Chemical Communications, 2015, 51, 10158-10161.	4.1	62
72	Dye-sensitized cobalt catalysts for high efficient visible light hydrogen evolution. International Journal of Hydrogen Energy, 2014, 39, 4836-4844.	7.1	61

#	Article	IF	CITATIONS
73	Facile synthesis of –Cî€N– linked covalent organic frameworks under ambient conditions. Chemical Communications, 2017, 53, 11956-11959.	4.1	61
74	Enhancing hydrogen generation via fabricating peroxide decomposition layer over NiSe/MnO2-CdS catalyst. Journal of Catalysis, 2018, 367, 269-282.	6.2	60
75	Pruning of the surface species on Ni/Al2O3 catalyst to selective production of hydrogen via acetone and acetic acid steam reforming. Applied Catalysis A: General, 2012, 427-428, 49-57.	4.3	58
76	The inhibition of hydrogen and oxygen recombination reaction by halogen atoms on over-all water splitting over Pt-TiO2 photocatalyst. Applied Catalysis B: Environmental, 2018, 236, 240-252.	20.2	58
77	Control growth of uniform platinum nanotubes and their catalytic properties for methanol electrooxidation. Electrochemistry Communications, 2009, 11, 45-49.	4.7	57
78	Carboxyl-assisted synthesis of Co nanorods with high energy facet on graphene oxide sheets for efficient photocatalytic hydrogen evolution. Applied Catalysis B: Environmental, 2017, 203, 789-797.	20.2	57
79	Enhancing photoactivity for hydrogen generation by electron tunneling via flip-flop hopping over iodinated graphitic carbon nitride. Applied Catalysis B: Environmental, 2017, 204, 33-42.	20.2	57
80	Water splitting over core-shell structural nanorod CdS@Cr2O3 catalyst by inhibition of H2-O2 recombination via removing nascent formed oxygen using perfluorodecalin. Applied Catalysis B: Environmental, 2018, 221, 618-625.	20.2	57
81	Syngas production by CO2 reforming of ethanol over Ni/Al2O3 catalyst. Catalysis Communications, 2009, 10, 1633-1637.	3.3	56
82	Water splitting by CdS/Pt/WO 3 -CeO x photocatalysts with assisting of artificial blood perfluorodecalin. Journal of Catalysis, 2017, 350, 189-196.	6.2	56
83	Partial Oxidation of Ethanol to Hydrogen over Ni–Fe Catalysts. Catalysis Letters, 2002, 81, 63-68.	2.6	53
84	Assembly of Ultraâ€Thin NiO Layer Over Zn _{1â^'<i>x</i>} Cd _{<i>x</i>} S for Stable Visibleâ€Light Photocatalytic Overall Water Splitting. ChemSusChem, 2019, 12, 1410-1420.	6.8	53
85	The long-term photocatalytic stability of Co2+-modified P25-TiO2 powders for the H2 production from aqueous ethanol solution. Journal of Photochemistry and Photobiology A: Chemistry, 2006, 181, 263-267.	3.9	52
86	Photocatalytic hydrogen generation using glycerol wastewater over Pt/TiO2. Frontiers of Chemistry in China: Selected Publications From Chinese Universities, 2009, 4, 32-38.	0.4	51
87	Direct conversion of Bi nanospheres into 3D flower-like BiOBr nanoarchitectures with enhanced photocatalytic properties. RSC Advances, 2014, 4, 583-586.	3.6	51
88	Visible-light-induced hydrogen production over Pt-Eosin Y catalysts with high surface area silica gel as matrix. Journal of Power Sources, 2007, 166, 74-79.	7.8	50
89	Investigation of the Effects of Molecular Structure on Oxygenated Hydrocarbon Steam Re-forming. Energy & Fuels, 2009, 23, 926-933.	5.1	49
90	Z-Scheme Photocatalytic System Utilizing Separate Reaction Centers by Directional Movement of Electrons. Journal of Physical Chemistry C, 2011, 115, 8586-8593.	3.1	49

#	Article	IF	CITATIONS
91	Photocatalytic hydrogen evolution under visible light irradiation by the polyoxometalate α-[AlSiW11(H2O)O39]5â^' -Eosin Y system. International Journal of Hydrogen Energy, 2012, 37, 12150-12157.	7.1	49
92	Renewable hydrogen production by a mild-temperature steam reforming of the model compound acetic acid derived from bio-oil. Journal of Molecular Catalysis A, 2012, 355, 123-133.	4.8	49
93	Interface Charge Transfer versus Surface Proton Reduction: Which Is More Pronounced on Photoinduced Hydrogen Generation over Sensitized Pt Cocatalyst on RGO?. Journal of Physical Chemistry C, 2015, 119, 13561-13568.	3.1	49
94	l-Arginine bearing an anthrylmethyl group: fluorescent molecular NAND logic gate with H+ and ATP as inputs. Tetrahedron Letters, 2007, 48, 3891-3894.	1.4	48
95	Enhanced surface electron transfer by fabricating a core/shell Ni@NiO cluster on TiO2 and its role on high efficient hydrogen generation under visible light irradiation. International Journal of Hydrogen Energy, 2014, 39, 8959-8968.	7.1	48
96	A novel amorphous CoSn _x O _y decorated graphene nanohybrid photocatalyst for highly efficient photocatalytic hydrogen evolution. Chemical Communications, 2014, 50, 5037-5039.	4.1	48
97	Catalytic oxidation of cyclohexane into cyclohexanol and cyclohexanone over a TiO2/TS-1 system by dioxygen under UV irradiation. Journal of the Chemical Society Chemical Communications, 1994, , 2423.	2.0	47
98	Size-controlled synthesis of colloidal platinum nanoparticles and their activity for the electrocatalytic oxidation of carbon monoxide. Journal of Colloid and Interface Science, 2005, 287, 159-166.	9.4	47
99	Direct electrochemistry and electrocatalysis of hybrid film assembled by polyelectrolyte–surfactant polymer, carbon nanotubes and hemoglobin. Journal of Electroanalytical Chemistry, 2006, 597, 51-59.	3.8	47
100	Dependence of Onset Potential for Methanol Electrocatalytic Oxidation on Steric Location of Active Center in Multicomponent Electrocatalysts. Journal of Physical Chemistry C, 2007, 111, 11897-11902.	3.1	47
101	Graft of lacunary Wells–Dawson heteropoly blue on the surface of TiO2 and its photocatalytic activity under visible light. Chemical Communications, 2009, , 3591.	4.1	47
102	BiAg Alloy Nanospheres: A New Photocatalyst for H ₂ Evolution from Water Splitting. ACS Applied Materials & Interfaces, 2014, 6, 19488-19493.	8.0	47
103	The roles of density-tunable surface oxygen vacancy over bouquet-like Bi2O3 in enhancing photocatalytic activity. Physical Chemistry Chemical Physics, 2014, 16, 4165.	2.8	47
104	Visible-to-ultraviolet Upconvertion: Energy transfer, material matrix, and synthesis strategies. Applied Catalysis B: Environmental, 2017, 206, 89-103.	20.2	47
105	Enhanced photocatalytic activity of Ag/Ag3PO4 coaxial hetero-nanowires. Journal of Materials Chemistry A, 2013, 1, 10612.	10.3	46
106	Modulating Photogenerated Electron Transfer and Hydrogen Production Rate by Controlling Surface Potential Energy on a Selectively Exposed Pt Facet on Pt/TiO2 for Enhancing Hydrogen Production. Journal of Physical Chemistry C, 2013, 117, 26415-26425.	3.1	46
107	Intrinsic magnetic characteristics-dependent charge transfer and visible photo-catalytic H ₂ evolution reaction (HER) properties of a Fe ₃ O ₄ @PPy@Pt catalyst. Chemical Communications, 2016, 52, 3038-3041.	4.1	46
108	High performance rare earth oxides LnOx (Ln=Sc, Y, La, Ce, Pr and Nd) modified Pt/C electrocatalysts for methanol electrooxidation. Journal of Power Sources, 2006, 162, 1067-1072.	7.8	45

#	Article	IF	CITATIONS
109	TiO ₂ Nanotube Arrays Modified with Crâ€Doped SrTiO ₃ Nanocubes for Highly Efficient Hydrogen Evolution under Visible Light. Chemistry - A European Journal, 2014, 20, 2654-2662.	3.3	45
110	Photo-catalytic H2 evolution over a series of Keggin-structure heteropoly blue sensitized Pt/TiO2 under visible light irradiation. Applied Surface Science, 2009, 255, 4378-4383.	6.1	44
111	Ion exchange synthesis of PAN/Ag ₃ PO ₄ core–shell nanofibers with enhanced photocatalytic properties. Journal of Materials Chemistry A, 2014, 2, 1668-1671.	10.3	44
112	High efficient solar hydrogen generation by modulation of Co-Ni sulfide (220) surface structure and adjusting adsorption hydrogen energy. Applied Catalysis B: Environmental, 2017, 206, 353-363.	20.2	44
113	Stable core–shell ZIF-8@ZIF-67 MOFs photocatalyst for highly efficient degradation of organic pollutant and hydrogen evolution. Journal of Materials Research, 2021, 36, 602-614.	2.6	44
114	Modification of TiO2 with sulfate and phosphate for enhanced eosin Y-sensitized hydrogen evolution under visible light illumination. Photochemical and Photobiological Sciences, 2013, 12, 1903-1910.	2.9	42
115	Promoted photoinduced charge separation and directional electron transfer over dispersible xanthene dyes sensitized graphene sheets for efficient solar H2 evolution. International Journal of Hydrogen Energy, 2013, 38, 2106-2116.	7.1	42
116	Influence of the pore structure of CeO2 supports on the surface texture and catalytic activity for CO oxidation. CrystEngComm, 2014, 16, 5189.	2.6	42
117	Inhibition of hydrogen and oxygen reverse recombination reaction over Pt/TiO2 by Fâ^' ions and its impact on the photocatalytic hydrogen formation. Journal of Catalysis, 2017, 353, 162-170.	6.2	42
118	Surface spintronics enhanced photo-catalytic hydrogen evolution: Mechanisms, strategies, challenges and future. Applied Surface Science, 2018, 434, 643-668.	6.1	42
119	Morphology-dependent activity of silver nanostructures towards the electro-oxidation of formaldehyde. Electrochemistry Communications, 2009, 11, 1255-1258.	4.7	41
120	Structural-Dependent Photoactivities of TiO ₂ Nanoribbon for Visible-Light-Induced H ₂ Evolution: The Roles of Nanocavities and Alternate Structures. Langmuir, 2010, 26, 447-455.	3.5	41
121	Improvement of Cu/Zn-based catalysts by nickel additive in methanol decomposition. Applied Catalysis A: General, 2002, 225, 77-86.	4.3	40
122	The spin-orbit coupling induced spin flip and its role in the enhancement of the photocatalytic hydrogen evolution over iodinated graphene oxide. Carbon, 2016, 108, 215-224.	10.3	39
123	Photosensitized reduction of water to hydrogen using novel Maya blue-like organic–inorganic hybrid material. Journal of Colloid and Interface Science, 2009, 333, 285-293.	9.4	38
124	NaCl-assisted low temperature synthesis of layered Zn-In-S photocatalyst with high visible-light activity for hydrogen evolution. RSC Advances, 2012, 2, 3458.	3.6	38
125	The dual functional roles of Ru as co-catalyst and stabilizer of dye for photocatalytic hydrogen evolution. International Journal of Hydrogen Energy, 2015, 40, 5824-5830.	7.1	38
126	Energy transfer in covalent organic frameworks for visible-light-induced hydrogen evolution. International Journal of Hydrogen Energy, 2019, 44, 11872-11876.	7.1	38

#	Article	IF	CITATIONS
127	Steam Reforming of Acetic Acid to Hydrogen over Fe–Co Catalyst. Chemistry Letters, 2006, 35, 452-453.	1.3	37
128	High efficient photocatalytic hydrogen evolution from formaldehyde over sensitized Ag@Ag-Pd alloy catalyst under visible light irradiation. Applied Catalysis B: Environmental, 2018, 237, 563-573.	20.2	37
129	The regulating effects of cobalt addition on the catalytic properties of silica-supported Ni–Co bimetallic catalysts for CO2 methanation. Reaction Kinetics, Mechanisms and Catalysis, 2014, 113, 101-113.	1.7	36
130	Modulating photogenerated electron transfer with selectively exposed Co–Mo facets on a novel amorphous g-C3N4/CoxMo1ⰒxS2 photocatalyst. RSC Advances, 2016, 6, 23709-23717.	3.6	36
131	A two-pronged strategy to enhance visible-light-driven overall water splitting via visible-to-ultraviolet upconversion coupling with hydrogen-oxygen recombination inhibition. Applied Catalysis B: Environmental, 2017, 212, 23-31.	20.2	36
132	Studies on photocatalytic activity of zinc ferrite catalysts synthesized by shock waves. Materials Research Bulletin, 1996, 31, 1049-1056.	5.2	35
133	High performance rare earth oxides LnOx (Ln=La, Ce, Nd, Sm and Dy)-modified Pt/SiO2 catalysts for CO oxidation in the presence of H2. Journal of Power Sources, 2008, 181, 120-126.	7.8	35
134	Hydrogen feed gas purification over bimetallic Cu–Pd catalysts – Effects of copper precursors on CO oxidation. International Journal of Hydrogen Energy, 2010, 35, 7253-7260.	7.1	35
135	Fabrication of Ag3PO4–PAN composite nanofibers for photocatalytic applications. CrystEngComm, 2013, 15, 4802.	2.6	35
136	lodide ions control galvanic replacement growth of uniform rhodium nanotubes at room temperature. Chemical Communications, 2008, , 6402.	4.1	34
137	An Anthracene-Based Chemosensor for Multiple Logic Operations at the Molecular Level. Journal of Physical Chemistry C, 2009, 113, 2541-2546.	3.1	34
138	NIR light driven catalytic hydrogen generation over semiconductor photocatalyst coupling up-conversion component. Applied Catalysis B: Environmental, 2019, 257, 117908.	20.2	33
139	The effect of plasma pre-treatment of carbon used as a Pt catalyst support for methanol electrooxidation. Carbon, 2007, 45, 41-46.	10.3	32
140	Composition, morphology and photocatalytic activity of Zn-In-S composite synthesized by a NaCl-assisted hydrothermal method. CrystEngComm, 2011, 13, 4770.	2.6	32
141	Fabrication and behaviors of CdS on Bi ₂ MoO ₆ thin film photoanodes. RSC Advances, 2017, 7, 10774-10781.	3.6	32
142	One pot synthesis of a highly efficient mesoporous ceria–titanium catalyst for selective catalytic reduction of NO. RSC Advances, 2016, 6, 76556-76567.	3.6	31
143	Oxidized multiwalled carbon nanotubes coated fibers for headspace solid-phase microextraction of amphetamine-type stimulants in human urine. Forensic Science International, 2018, 290, 49-55.	2.2	31
144	Size effect of gold nanoparticles on the electrocatalytic oxidation of carbon monoxide in alkaline solution. Journal of Nanoparticle Research, 2007, 9, 1145-1151.	1.9	29

#	Article	IF	CITATIONS
145	Morphological controlled synthesis and catalytic activities of gold nanocrystals. Materials Letters, 2008, 62, 2696-2699.	2.6	29
146	Improving catalytic activity and stability by in-situ regeneration of Ni-based catalyst for hydrogen production from ethanol steam reforming via controlling of active species dispersion. International Journal of Hydrogen Energy, 2016, 41, 13993-14002.	7.1	29
147	The effect of K addition on Au/activated carbon for CO selective oxidation in hydrogen-rich gas. Catalysis Letters, 2007, 115, 46-51.	2.6	27
148	Controlled synthesis of pentagonal gold nanotubes at room temperature. Nanotechnology, 2008, 19, 275306.	2.6	27
149	Electrocatalytic oxidation of carbon monoxide on platinum-modified polyaniline film electrodes. Thin Solid Films, 2006, 497, 309-314.	1.8	26
150	Synthesis and characterization of high performance Pt-(PrxCeyOz)/C catalysts for methanol electrooxidation. Applied Catalysis B: Environmental, 2008, 79, 1-7.	20.2	26
151	Hydrogen Evolution Over Heteropoly Blue-Sensitized Pt/TiO2 Under Visible Light Irradiation. Catalysis Letters, 2009, 127, 319-322.	2.6	26
152	Efficient generation of hydrogen from biomass without carbon monoxide at room temperature – Formaldehyde to hydrogen catalyzed by Ag nanocrystals. International Journal of Hydrogen Energy, 2010, 35, 7177-7182.	7.1	25
153	Construction of Möbius-strip-like graphene for highly efficient charge transfer and high active hydrogen evolution. Journal of Catalysis, 2017, 354, 258-269.	6.2	25
154	Visible light driven water splitting over CaTiO3/Pr3+-Y2SiO5/RGO catalyst in reactor equipped artificial gill. Applied Catalysis B: Environmental, 2018, 224, 553-562.	20.2	25
155	Research Progresses in the Preparation of Co-based Catalyst Derived from Co-MOFs and Application in the Catalytic Oxidation Reaction. Catalysis Surveys From Asia, 2019, 23, 64-89.	2.6	25
156	The activity enhancement of photocatalytic water splitting by F- pre-occupation on Pt(100) and Pt(111) co-catalyst facets. Applied Catalysis B: Environmental, 2020, 266, 118647.	20.2	25
157	New evidence for the regulation of photogenerated electron transfer on surface potential energy controlled co-catalyst on TiO2 – The investigation of hydrogen production over selectively exposed Au facet on Au/TiO2. International Journal of Hydrogen Energy, 2014, 39, 7672-7685.	7.1	24
158	Highly efficient hydrogen production from formaldehyde over Ag/γ-Al2O3 catalyst at room temperature. International Journal of Hydrogen Energy, 2014, 39, 9114-9120.	7.1	24
159	Enhanced Catalytic Performance of Three-Dimensional Ordered Mesoporous Transition Metal (Co, Cu,) Tj ETQq1 I	L 0.78431	4 rgBT /Ove
160	Noble-metal-free NiSn x O y decorated graphene cocatalyst for highly efficient reduction of water toÂhydrogen. International Journal of Hydrogen Energy, 2015, 40, 9634-9641.	7.1	24
161	Fivefold Enhanced Photoelectrochemical Properties of ZnO Nanowire Arrays Modified with C3N4 Quantum Dots. Catalysts, 2017, 7, 99.	3.5	24
162	Controlled synthesis and photocatalytic investigation of different-shaped one-dimensional titanic acid nanomaterials. Journal of Power Sources, 2008, 185, 577-583.	7.8	23

#	Article	IF	CITATIONS
163	Steam reforming of bio-oil derived small organics over the Ni/Al2O3 catalyst prepared by an impregnation–reduction method. Catalysis Communications, 2014, 55, 74-77.	3.3	23
164	The roles of various Ni species over SnO2 in enhancing the photocatalytic properties for hydrogen generation under visible light irradiation. Applied Surface Science, 2014, 305, 235-241.	6.1	23
165	Recent Progress on Establishing Structure–Activity Relationship of Catalysts for Selective Catalytic Reduction (SCR) of NOx with NH3. Catalysis Surveys From Asia, 2018, 22, 1-19.	2.6	23
166	High performance phosphorus-modified ZSM-5 zeolite for butene catalytic cracking. Korean Journal of Chemical Engineering, 2010, 27, 812-815.	2.7	22
167	Visible light induced CO2 reduction and Rh B decolorization over electrostatic-assembled AgBr/palygorskite. Journal of Colloid and Interface Science, 2012, 377, 277-283.	9.4	22
168	Rhodium tin composite oxides co-catalyst for high efficient photocatalytic hydrogen evolution. International Journal of Hydrogen Energy, 2015, 40, 9061-9068.	7.1	22
169	Graphene-induced spatial charge separation for selective water splitting over TiO2 photocatalyst. Catalysis Communications, 2016, 80, 28-32.	3.3	22
170	Steam reforming of acetic acid over Cu Zn Co catalyst for hydrogen generation: Synergistic effects of the metal species. International Journal of Hydrogen Energy, 2016, 41, 13960-13969.	7.1	21
171	Behavior of borate complex anion on the stabilities and the hydrogen evolutions of ZnxCo3â~'xO4 decorated graphene. Superlattices and Microstructures, 2015, 82, 599-611.	3.1	20
172	The enhancement of electron transportation and photo-catalytic activity for hydrogen generation by introducing spin-polarized current into dye-sensitized photo-catalyst. Catalysis Science and Technology, 2016, 6, 7693-7697.	4.1	20
173	Homostructural Ta3N5 nanotube/nanoparticle photoanodes for highly efficient solar-driven water splitting. Applied Catalysis B: Environmental, 2020, 277, 119217.	20.2	20
174	Fe2S2 nano-clusters catalyze water splitting by removing formed oxygen using aid of an artificial gill under visible light. Journal of Catalysis, 2017, 352, 572-578.	6.2	19
175	Enhancing photoactivity for hydrogen generation by electron tunneling via flip-flop hopping over Möbius strip-like RGO. Applied Catalysis B: Environmental, 2017, 219, 501-510.	20.2	19
176	Morphology-controlled Preparation of Silver Nanocrystals and Their Application in Catalysis. Chemistry Letters, 2008, 37, 514-515.	1.3	18
177	Tunable photocatalytic selectivity and stability of Ba-doped Ag3PO4 hollow nanosheets. Chinese Journal of Catalysis, 2015, 36, 1587-1595.	14.0	18
178	Significant Effect of Pressure on the H2 Releasing from Photothermal-Catalytic Water Steam Splitting over TiSi2 and Pt/TiO2. Catalysis Letters, 2008, 125, 376-379.	2.6	17
179	Graphene supported Co–Mo–P catalyst for efficient photocatalyzed hydrogen generation. International Journal of Hydrogen Energy, 2016, 41, 6706-6712.	7.1	17
180	A molecular half-subtractor based on a fluorescence and absorption dual-modal sensor for copper ions. Tetrahedron Letters, 2008, 49, 5676-5679.	1.4	16

#	Article	IF	CITATIONS
181	The Inhibition Effect of Potassium Addition on Methane Formation in Steam Reforming of Acetic Acid over Alumina-supported Cobalt Catalysts. Chemistry Letters, 2008, 37, 614-615.	1.3	16
182	Enhancing water splitting activity by protecting hydrogen evolution activity site from poisoning of oxygen species. Applied Catalysis B: Environmental, 2019, 249, 138-146.	20.2	16
183	980 nm NIR light driven overall water splitting over a combined CdS–RGO–NaYF ₄ –Yb ³⁺ /Er ³⁺ photocatalyst. Catalysis Science and Technology, 2020, 10, 2389-2397.	4.1	16
184	Promotion effect of lanthanum addition on the catalytic activity of zirconia supported platinum and tungstophosphoric acid catalyst for n-pentane isomerization. Applied Surface Science, 2009, 255, 6504-6507.	6.1	15
185	Enhancement of Pt–Ru catalytic activity for catalytic wet air oxidation of methylamine via tuning the Ru surface chemical state and dispersion by Pt addition. RSC Advances, 2014, 4, 15325-15331.	3.6	15
186	Influence of pore structures of a carbon support on the surface textures of a CO oxidation catalyst. RSC Advances, 2015, 5, 59666-59676.	3.6	15
187	Structural and Textural Characteristics of Zn-Containing ZSM-5 Zeolites and Application for the Selective Catalytic Reduction of NOx with NH3 at High Temperatures. Catalysis Surveys From Asia, 2016, 20, 41-52.	2.6	15
188	Synthesis and properties of strontium ferrite ultrafine powders. Journal of Materials Science Letters, 1996, 15, 397-399.	0.5	15
189	Influence of hydrogen bonds on charge distribution and conformation of l-arginine. Spectrochimica Acta - Part A: Molecular and Biomolecular Spectroscopy, 2007, 67, 368-371.	3.9	14
190	Three-input chemical logic circuits based on a new fluorescent sensor for ATP and Cu2+in aqueous solution. Sensors and Actuators B: Chemical, 2008, 133, 617-621.	7.8	14
191	Regulating Role of Cobalt Oxide on Deleterious Chlorine Ion over PdO/SiO ₂ for CO Oxidation. Journal of Physical Chemistry C, 2009, 113, 17070-17075.	3.1	14
192	Ln _{<i>x</i>} Pd _{<i>y</i>} Ti _{1â^'<i>x</i>â^'<i>y</i>} O ₆ Catalysts: Formation of Oxygen Vacancy and Identification of the Active Site for CO Oxidation. Journal of Physical Chemistry C, 2009, 113, 4161-4167.	3.1	14
193	Enhanced Surface Electron Transfer with the Aid of Methyl Viologen on the Co ₃ O ₄ -g-C ₃ N ₄ Photocatalyst. Chemistry Letters, 2016, 45, 116-118.	1.3	14
194	Inhibition of hydrogen and oxygen recombination over amide–functionalized graphene and the enhancement of photocatalytic hydrogen generation in dye–sensitized AF–RGO/Pt photocatalyst dispersion. Applied Catalysis B: Environmental, 2018, 232, 371-383.	20.2	14
195	TiO ₂ protection layer and well-matched interfaces enhance the stability of Cu ₂ ZnSnS ₄ /CdS/TiO ₂ for visible light driven water splitting. Catalysis Science and Technology, 2021, 11, 5505-5517.	4.1	14
196	Preparation of SiO2-Pt-CdS composite photocatalyst and its photocatalytic activity for hydrogen evolution under visible light. Reaction Kinetics and Catalysis Letters, 2008, 95, 185-192.	0.6	13
197	Hard-template synthesis of three-dimensional mesoporous Cu–Ce based catalysts with tunable architectures and their application in the CO catalytic oxidation. RSC Advances, 2016, 6, 64247-64257.	3.6	13
198	Inhibition of the excited-state Rose Bengal (RB) nonradiative process by introducing DMSO for highly efficient photocatalytic hydrogen evolution. RSC Advances, 2016, 6, 29538-29544.	3.6	13

#	Article	IF	CITATIONS
199	Co–P/graphene alloy catalysts doped with Cu and Ni for efficient photocatalytic hydrogen generation. New Journal of Chemistry, 2017, 41, 13804-13811.	2.8	13
200	Controlled Synthesis of TiO2 Shape and Effect on the Catalytic Performance for Selective Catalytic Reduction of NOx with NH3. Catalysis Surveys From Asia, 2018, 22, 105-117.	2.6	13
201	Hydrogen generation from toxic formaldehyde catalyzed by low-cost Pd–Sn alloys driven by visible light. Journal of Materials Chemistry A, 2020, 8, 9616-9628.	10.3	13
202	A new method to construct hierarchical ZSM-5 zeolites with excellent catalytic activity. Journal of Porous Materials, 2014, 21, 957-965.	2.6	12
203	Modulation of HCHO, H2O and H adsorption on AgPd cocatalyst by optimizing of selective exposed facet to enhancing the efficiency of conversion toxic formaldehyde into hydrogen driven by visible light. Journal of Catalysis, 2019, 375, 493-506.	6.2	12
204	pH induced size-selected synthesis of PtRu nanoparticles, their characterization and electrocatalytic properties. Journal of Molecular Catalysis A, 2007, 265, 42-49.	4.8	11
205	Study of One Step Synthesis of Rare Earth Zeolite (Ln–ZSM-5) and Application for Low Temperature CO Catalytic Oxidation. Catalysis Surveys From Asia, 2013, 17, 147-155.	2.6	11
206	Skeletal Isomerization of n-Pentane over Platinum-Promoted Tungstophosphoric Acid Supported on MCM-41. Catalysis Letters, 2008, 125, 83-89.	2.6	10
207	Differential effects of Mg(ii) and Nα-4-tosyl-l-arginine methyl ester hydrochloride on the recognition and catalysis in ATP hydrolysis. Dalton Transactions, 2008, , 1081-1086.	3.3	10
208	Photocatalytic Materials. International Journal of Photoenergy, 2012, 2012, 1-5.	2.5	10
209	Effect of Different Pore Structures on the Surface Textures of the Cu-Doped CeO2 Catalysts and Applied for CO Catalytic Oxidation. Catalysis Surveys From Asia, 2015, 19, 129-139.	2.6	10
210	Enantiomer-selective sensing and the light response of chiral molecules coated with a persistent luminescent material. Chemical Communications, 2019, 55, 13390-13393.	4.1	10
211	Control Reaction Path of CO Oxidation by Regulating the Oxidation State of Au Species. Catalysis Letters, 2010, 134, 72-77.	2.6	8
212	Surface texture and physicochemical characterization of mesoporous carbon – wrapped Pd–Fe catalysts for low-temperature CO catalytic oxidation. Physical Chemistry Chemical Physics, 2015, 17, 29027-29035.	2.8	8
213	Epoxidation of β-ionone using molecular oxygen over Pt/MCM-41 catalyst under mild conditions. Catalysis Letters, 2007, 117, 126-129.	2.6	7
214	A Highly Effective Pt and H3PW12O40 Modified Zirconium Oxide Metal–Acid Bifunctional Catalyst for Skeletal Isomerization: Preparation, Characterization and Catalytic Behavior Study. Catalysis Letters, 2008, 125, 340-347.	2.6	7
215	Spectroscopy study on the noncovalent interactions in the binary and ternary systems of I-lysine, adenosine 5′-triphosphate and magnesium ions. Spectrochimica Acta - Part A: Molecular and Biomolecular Spectroscopy, 2011, 78, 1305-1309.	3.9	7
216	Low temperature carbon monoxide catalytic oxidation at the Pd/Ce–Zr–Al–Ox catalyst. Journal of Sol-Gel Science and Technology, 2013, 66, 526-532.	2.4	7

#	Article	IF	CITATIONS
217	Deposition of Pd–Fe nanoparticles onto carbon spheres with controllable diameters and applied for CO catalytic oxidation. RSC Advances, 2014, 4, 23262-23270.	3.6	7
218	High-temperature steam reforming of bio-oil derived light organics and methane to hydrogen-rich gas with trace CO via rational temperature control. RSC Advances, 2014, 4, 18924-18929.	3.6	7
219	Study of catalytic activity and product selectivity of M/Al2O3-CeO2 (M = Pt-Ru, Ru, and Pt) in catalytic wet air oxidation of methylamine. Chinese Journal of Catalysis, 2014, 35, 1212-1223.	14.0	7
220	Synthesis of High Dispersion and Uniform Nano-sized Flame Retardant-Used Hexagonal Mg(OH)2. Journal of Cluster Science, 2016, 27, 1831-1841.	3.3	7
221	Ultrasonic assisted rapid synthesis of high uniform super-paramagnetic microspheres with core-shell structure and robust magneto-chromatic ability. Journal of Magnetism and Magnetic Materials, 2017, 426, 1-10.	2.3	7
222	Improved Light Harvesting and Efficiency for Overall Water Splitting by Embedding TiO ₂ Transition Layer in GaP/Ga ₂ O ₃ /Ga ₂ Se ₃ Multijunction Photocatalyst. Solar Rrl, 2021, 5, 2000619.	5.8	7
223	Kinetic and mechanism study on photocatalytic detoxification of Cr(VI) ions on TiO ₂ catalyst. Toxicological and Environmental Chemistry, 1999, 70, 333-347.	1.2	6
224	Butene catalytic cracking to ethylene and propylene on fluorinated ZSM-5-based catalyst. Reaction Kinetics, Mechanisms and Catalysis, 2013, 108, 231-239.	1.7	6
225	Ice core dust particulate by XPS-SEM/EDAX. Science Bulletin, 1999, 44, 1424-1427.	1.7	5
226	Interaction of cationic vesicle with ribonucleotides (AMP, ADP, and ATP) and physicochemical characterization of DODAB/ribonucleotides complexes. Biophysical Chemistry, 2007, 127, 19-27.	2.8	4
227	The Evidences of Morphology Dependent Electroactivity Toward CO Oxidation over Bismuth Oxide Supported Pt. Catalysis Letters, 2010, 135, 114-119.	2.6	4
228	Preparation of Co-Pd bimetallic nanoparticles encapsulated in bamboo-like N-doped mesoporous carbon by a facile one-pot method for green Suzuki coupling. Research on Chemical Intermediates, 2019, 45, 3809-3821.	2.7	4
229	Generation of enhanced stability of SnO/In(OH)3/InP for photocatalytic water splitting by SnO protection layer. Frontiers in Energy, 2021, 15, 710-720.	2.3	4
230	Boron substitution enhanced activity of BxGa1â^'xAs/GaAs photocatalyst for water splitting. Applied Catalysis B: Environmental, 2022, 300, 120690.	20.2	4
231	The Support Effect over Pt–H3PW12O40 Based Metal-Acid Bifunctional Catalysts on the Catalytic Performance in n-Pentane Isomerization. Catalysis Letters, 2009, 129, 215-221.	2.6	3
232	Catalytic wet oxidation of aqueous methylamine: comparative study on the catalytic performance of platinum–ruthenium, platinum, and ruthenium catalysts supported on titania. Environmental Technology (United Kingdom), 2015, 36, 1160-1166.	2.2	3
233	Preparation and Catalytic Activity of Two-dimensionally Networked Gold Nanowires. Chemistry Letters, 2006, 35, 914-915.	1.3	2
234	A Calcium(II)-Based l-Arginine for ATP Binding and Hydrolysis. Journal of Inorganic and Organometallic Polymers and Materials, 2008, 18, 435-440.	3.7	2

0

#	Article	IF	CITATIONS
235	Pivotal Role of Chirality in Photoelectrocatalytic (PEC) Water Splitting. Current Chinese Science, 2021, 1, 115-121.	0.5	1

Seizing solar hydrogen from water promoted by magic spin transporting, chiral-induced spin state–selective filtering, and upconversion. , 2020, , 191-209.